

- Pichavaram mangrove wetland using remote sensing data. *Curr. Sci.*, 2003, **85**, 794–798.
22. Paling, E. I., Kobryn, H. T. and Humphreys, G., Assessing the extent of mangrove change caused by cyclone Vance in the eastern Exmouth Gulf, northwestern Australia. *Estuarine, Coastal Shelf Sci.*, 2008, **77**, 603–613.
  23. Giri, C., Pengra, B., Zhu, Z., Singh, A. and Tieszen, L., Monitoring mangrove forest dynamics of the Sundarbans in Bangladesh and India using multi-temporal satellite data from 1973 to 2000. *Estuarine, Coastal Shelf Sci.*, 2007, **73**, 91–100.
  24. Mas, J. F., Mapping land use/cover in a tropical coastal area using satellite sensor data, GIS and artificial neural networks. *Estuarine, Coastal Shelf Sci.*, 2004, **59**, 219–230.
  25. Myint, S. W., Giri, C. P., Wang, L., Zhu, Z. and Gillette, S. C., Identifying mangrove species and their surrounding land use and land cover classes using an object-oriented approach with a lacunarity spatial measure. *GISci. Remote Sensing*, 2008, **45**, 188–208.
  26. Wang, L., Sousa, W. and Gong, P., Integration of object-based and pixel-based classification for mangrove mapping with IKONOS imagery. *Int. J. Remote Sensing*, 2004, **25**, 5655–5668.
  27. Green, E. P., Clear, C. D., Mumby, P. J., Edwards, A. J. and Ellis, A. C., Remote sensing techniques for mangrove mapping. *Int. J. Remote Sensing*, 1998, **19**, 935–956.
  28. Jensen, J. R., Lin, H., Yang, X., Ramset, E., Davis, B. A. and Thoenke, C. W., The measurement of mangrove characteristics in south-west Florida using SPOT multispectral data. *Geocartogr. Int.*, 1991, **2**, 13–21.
  29. National Wetland Atlas, SAC/EPASA/ABHG/NWIA/ATLAS/34/2011, Space Applications Centre (ISRO), Ahmedabad, India, 2011; <http://moef.nic.in/downloads/public-information/NWIA-Assam Atlas.pdf> (accessed on 6 January 2013).
  30. Sushma Panigrahy, Murthy, T. V. R., Patel, J. G. and Singh, T. S., Wetlands of India: inventory and assessment at 1 : 50,000 scale using geospatial techniques. *Curr. Sci.*, 2012, **102**, 852–856.
  31. Crist, E. P. and Cicone, R. C., Application of the tasseled cap concept to simulated Thematic Mapper data. *Photogramm. Eng. Remote Sensing*, 1984, **50**, 343–352.
  32. Liang, S., Liu, J. and Liang, M., Ecological study on the mangrove communities in Beilunhekou National Nature Reserve. *J. Guangxi Normal University*, 2004, **22**, 70–76.
  33. <http://port.shippingchina.com/tide/index/> (accessed on 6 January 2013).
  34. Chander, G. and Markham, B., Revised Landsat-5 TM radiometric calibration procedures and postcalibration dynamic ranges. *IEEE Trans. Geosci. Remote Sensing*, 2003, **41**, 2674–2677.
  35. Thenkabail, P. S., Enclona, E. A., Ashton, M. S., Legg, C. and Dieu, M. J. D., Hyperion, IKONOS, ALI, and ETM+ sensors in the study of African rainforests. *Remote Sensing Environ.*, 2004, **90**, 23–43.
  36. Chavez, P. S., An improved dark-object subtraction technique for atmospheric scattering correction of multispectral data. *Remote Sensing Environ.*, 1986, **24**, 459–479.
  37. Chavez, P. S., Image-based atmospheric corrections – revisited and improved. *Photogramm. Eng. Remote Sensing*, 1996, **62**, 1025–1036.
  38. Kaufman, Y. and Remer, L., Detection of forests using mid-IR reflectance: an application for aerosol studies. *IEEE Trans. Geosci. Remote*, 1994, **32**, 672–683.

**ACKNOWLEDGEMENTS.** This study was supported by the National Natural Science Foundation of China (Grant No. 41201461), the National Science and Technology Major Project (Grant No. 30-Y20A01-9003-12/13, China) and the project funded by the Priority Academic Programme Development of Jiangsu Higher Education Institutions.

Received 10 May 2013; accepted 17 May 2013

## The Delhi 1960 earthquake: epicentre, depth and magnitude

S. K. Singh<sup>1\*</sup>, G. Suresh<sup>2</sup>, R. S. Dattatrayam<sup>2</sup>,  
H. P. Shukla<sup>2</sup>, S. Martin<sup>3</sup>, J. Havskov<sup>4</sup>,  
X. Pérez-Campos<sup>1</sup> and A. Iglesias<sup>1</sup>

<sup>1</sup>Instituto de Geofísica, Universidad Nacional Autónoma de México, Ciudad Universitaria, 04510 México, DF, México

<sup>2</sup>India Meteorological Department, Lodi Road, New Delhi 110 003, India

<sup>3</sup>Victoria University of Wellington, School of Geography, Environment and Earth Sciences, Wellington, New Zealand

<sup>4</sup>Department of Earth Sciences, University of Bergen, Bergen, Norway

**Though the Delhi earthquake of 27 August 1960 is important in understanding seismic hazard to the city, there is large uncertainty associated with its reported epicentre, depth and magnitude. The reported epicentres given in different catalogues are not consistent with felt and damage reports, and the depths (58–109 km) are also inconsistent with recorded waveforms (including the excitation of *Lg* waves), decay of seismic intensities with distance, number of after-shocks, earthquake sound and seismotectonics of the region. The reported magnitude of the earthquake varies between 5.3 and 6.0. We have performed an exhaustive analysis of the available information, including comparison of the seismograms of the 1960 earthquake with six recent well-recorded events as well as with the Moradabad earthquake of 1966. We find that: (1) A more reliable epicentre as compared to the instrumentally determined one, is provided by the locus of the strongest seismic intensity: 28.47°N, 77.00°E (between Delhi Cantonment and Gurgaon). (2) The earthquake was shallow (depth  $\leq 30$  km, but most likely  $\leq 15$  km). (3) The magnitude of the earthquake was  $M_w$  4.8 (range  $M_w$  4.6–4.9). The seismic intensity is also consistent with  $M_w < 5.0$ . We conclude that the Delhi 1960 earthquake occurred between Delhi Cantonment and Gurgaon, it was shallow and its magnitude was 4.8, significantly less than  $M$  6.0 often used in studies dealing with hazard in the city.**

**Keywords:** Earthquake, epicentre, depth, magnitude, seismic hazard.

THE National Capital Territory (NCT) of Delhi, presently home to more than 16 million people, is vulnerable to earthquakes at local and regional distances as well as to great earthquakes along the Himalayan arc. Unfortunately, the information on historical seismicity in the NCT is plagued with large uncertainty. There appear to be two previous local earthquakes that were damaging. However, the location and magnitude of neither of these events are well constrained. The first one caused numerous fatalities

\*For correspondence. (e-mail: krishnamex@yahoo.com)

and damage within the environs of Old Delhi<sup>1</sup> on Jom'e, 22 Ramazan 1132 AH that corresponds to the Gregorian date (New Style) of Friday, 26 July 1720. A translation of this account is available, along with a Julian date (Old Style)<sup>2</sup> of 15 July 1720 that is often erroneously mistaken for a New Style date. The second earthquake occurred on the morning of Sunday, 20 December 1835. It was 'clearly perceptible and felt to an alarming degree by some of the inhabitants, residing at the Western precincts' (Delhi Gazette, 30 December 1835). 'It resulted in an unknown number of deaths in the city and some damage at the British Residency north of Kashmiri Gate....'<sup>3</sup> However, despite the intensity in the NCT, it was not perceptible beyond Meerut (India Gazette, 8 January 1836).

A popular misconception is associated with the earthquake of 1 September 1803, which damaged many towns in the Gangetic Plains, including Mathura and also dislodged the upper parts of the Qutub Minar in Delhi<sup>2</sup>. Bapat *et al.*<sup>4</sup> assigned it an intensity of MM IX with an epicentre near Mathura. This was subsequently converted to a magnitude<sup>5</sup>. Later investigations using first-hand historical documents<sup>6</sup>, as well as intensity attenuation scaling relations, recalculated the magnitude and relocated this earthquake in the Kumaon Himalayas<sup>7</sup>. Nonetheless, an erroneous location for this event continues to appear in contemporary listings and it continues to be included in some studies of the seismicity of the Delhi region as a local event.

The Delhi earthquake of 27 August 1960 is the largest instrumentally recorded event in and near the NCT. For this reason, it is one of the critical-scenario earthquakes in the estimation of seismic hazard of the NCT. Yet the epicentre, depth and magnitude of the earthquake are uncertain. No seismograph was in operation in Delhi at the time of the earthquake. Dehradun (epicentral distance ~185 km) was the closest station which recorded the event. The United States Coast and Geodetic Survey (USCGS) reported its epicentre as 28.2°N, 77.4°E and depth  $H$  as 109 km. Based on the excitation of  $Lg$  waves and emergent nature of  $P$  waves on regional seismograms, Saha<sup>8</sup> argued for a shallow focus. He also reported a magnitude of ~6 from the recordings at Shillong seismological observatory without specifying the seismogram(s) used in the estimation. Rothe's catalogue<sup>9</sup> lists the location as 28.6°N, 76.7°E,  $H = 58$  km. The magnitude is assigned as  $d$ , i.e. between 5.3 and 5.8. The International Seismological Summary (ISS) bulletin does not list the earthquake at all. The epicentre and magnitude of the event listed in the catalogue of earthquakes in India<sup>10</sup> is from USCGS and Saha<sup>7</sup> respectively. Several papers dealing with ground-motion estimation and seismic hazard in Delhi take  $M 6$  as the magnitude of the earthquake<sup>11-15</sup>.

An extensive report on the earthquake, which included description of the damage and an isoseismal map, was

prepared by Nath *et al.*<sup>16</sup>. Damage occurred at Delhi Cantonment, Gurgaon, Palam and in villages between Gurgaon and Delhi. Elsewhere in Delhi, several buildings developed cracks, including Kotla Gumbaj, Rashtrapati Bhavan, Red Fort and the Ashoka Hotel. From field observations, it was suggested that the focus was shallow (5–6 km) and the epicentre was located between Delhi Cantonment and Gurgaon<sup>15</sup>. The modified Mercalli intensity (MMI) in the epicentral area was VII. Five felt aftershocks were reported in the next two weeks. The main shock and at least one of the aftershocks were accompanied by rumbling or booming sound<sup>16</sup>. Two persons died and about 100 persons sustained minor injuries by falling debris, in stampedes or after leaping from the upper floors of buildings in panic (*The Tribune*, 29 August 1960). The report mentions that 75% of the buildings in the epicentral area developed hair-pin to half-inch cracks. This earthquake was felt in many parts of North India, including Ghaziabad, Jaipur, Kanpur and Meerut<sup>17</sup>.

In view of the importance of the 1960 earthquake in the estimation of seismic hazard of Delhi, we re-examine damage and felt reports and regional seismograms of the event to estimate its location and magnitude. The magnitude and depth estimation rely heavily on comparison of seismograms of the 1960 earthquake with those from recent, well-studied earthquakes as well as the 1966 Moradabad ( $m_b$  5.6) earthquake.

Due to lack of adequate coverage and poor quality of seismograms, it is not possible to determine an accurate instrumental epicentre of the 1960 earthquake based on phase data. The affected region was well populated. For this reason, we think that a more accurate epicentre (with an error of probably ~5 km) is given by the centre of the contour of maximum intensity<sup>16</sup> (28.47°N, 77.00°E) than the one determined from the phase data. This location is 49 km to the N53°W of USCGS epicentre and 33 km to the S64°E of Rothe's epicentre<sup>9</sup>.

As for depth, there are several arguments in favour of it being shallow: (1) Relative excitation of  $Lg$  waves and emergent nature of  $P$  waves on regional seismograms<sup>8</sup>. (2) Seismicity and tectonics of the area. (3) Decay of seismic intensity with distance. (4) Reports of aftershocks, and booming and rumbling sound during the main shock and, at least, one aftershock<sup>16</sup>. The excitation of  $Lg$  waves and, hence, shallow depth of the 1960 earthquake is discussed by Saha<sup>8</sup>. Below we compare synthetic and observed seismograms of the 1960 earthquake. As we show this comparison supports a shallow source. Although well-located, recent earthquakes in the region are mostly shallow ( $H \leq 15$  km), an event at depth of 30 km has been reliably located in the area<sup>18</sup>. There is no well-located recent earthquake occurring at greater depth. Tectonically, a mantle earthquake in this region would be very unusual. The rapid decay of seismic intensities argues for a shallow depth (see below). The number of aftershocks and reports of booming and rumbling sound

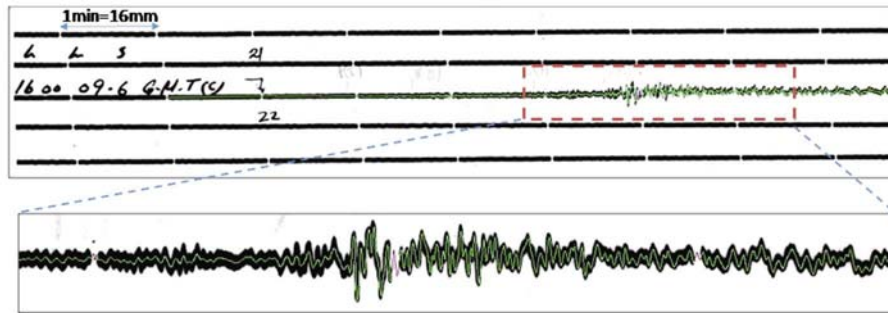


**Figure 1.** (Top) A portion of scanned (600 dpi) Milne–Shaw EW seismogram of Delhi 1960 earthquake recorded at Chatra (CHA), Nepal. On the original seismograms 1 min = 16 mm. The digitized seismogram (in green) is superimposed on the scanned one. (Bottom) An enlargement of the digitized seismogram superimposed on the scanned one.

are also indicative of shallow, crustal rather than mantle-depth of the source. We note, however, that argument (4) is not definitive. It is true that generally shallower earthquakes give rise to more aftershocks than the deeper ones. But the reported five aftershocks are not too many to completely discount a deeper source. All published reports on earthquake sound are associated with shallow sources (see for example, Michael<sup>19</sup> for a review). These sounds are related to ground motion in the frequency range<sup>20</sup> 20–50 Hz. However, there is no theoretical reason why a deeper event cannot be heard if the magnitude is sufficiently large, especially since attenuation at depth may be lower. In short, while individual arguments above supporting shallow depth may not be conclusive, taken together they point to a shallow depth for the 1960 earthquake.

The earthquake was recorded by several seismic observatories operated by the India Meteorological Department (IMD). At present, the following recordings are available in the IMD archives: seismograms recorded by (a) Wood–Anderson seismographs at Toklai ( $\Delta \sim 1705$  km) and Vizianagaram ( $\Delta \sim 1319$  km), (b) Sprengnether micro-seismographs at Shillong ( $\Delta \sim 1510$  km) and Poona ( $\Delta \sim 1146$  km) and (c) Milne–Shaw seismographs at Bokaro Thermal ( $\Delta \sim 1027$  km), Poona ( $\Delta \sim 1146$  km) and Chatra ( $\Delta \sim 1051$  km). We refrain from using Wood–Anderson seismographs to compute local magnitude  $M_L$  because an appropriate attenuation curve ( $-\log A_0$  term in the Richter’s definition of  $M_L$ ) has not been developed for India. Use of Southern California attenuation curve, especially extrapolated to such large distances ( $> 1300$  km), would result in gross overestimation of magnitude because of high  $Q$  of the Indian shield. We could not find reliable response curves of the Sprengnether seismographs. However, we found the Shillong EW seismogram (the only horizontal component available) most useful since we could compare the 1960 recording with those of the 1966 Moradabad earthquake whose magnitude is known ( $m_b$  5.6).

We first consider the recordings of the Milne–Shaw seismographs, deferring the analysis of Shillong Spreng-

nether seismogram. The instrumental constants of the Milne–Shaw seismograph are: pendulum period = 12.0 s, static magnification = 250, damping ratio = 20 (damping constant = 0.690). Thus, the response of the system is flat for displacement at frequencies  $f$  greater than about 0.1 Hz and falls off as  $f^{-2}$  at smaller  $f$ . Both horizontal records are available at Bokaro Thermal and Chatra. At Poona, only NS component is available. In the following, we will denote Bokaro Thermal, Poona, Chatra and Shillong by BOKR, PUNE, CHA and SHL respectively.

The analogue seismograms were digitized following the procedure described in Pintore *et al.*<sup>21</sup> and re-sampled at equal time interval. Figure 1 illustrates scanned EW CHA record over which the digitized seismogram has been superimposed. Figures 2–4 show displacement seismograms at BOKR, PUNE (NS components), and CHA (EW component) respectively. To infer the depth of the 1960 earthquake, we compare its waveforms at BOKR and PUNE with two recent, well-studied Delhi earthquakes (25 November 2007 and 5 March 2012, Table 1) recorded at the same stations by broadband seismographs. The high-pass (at 0.1 Hz) displacement seismograms of the recent earthquakes are also plotted in Figures 2 and 3. At BOKR, the seismogram of the 1960 earthquake is similar to that of the 2007 ( $H = 30$  km) event. At PUNE, however, the 1960 earthquake bears more resemblance with the 2012 ( $H = 15$  km) earthquake. The comparison suggests a depth between 15 and 30 km for the 1960 earthquake.

To further check whether the hypocentre of the 1960 earthquake could have been deeper in the mantle, we generated synthetic seismograms at BOKR and PUNE using discrete wavenumber algorithm<sup>22</sup> corresponding to an  $M_w$  4.8 earthquake located at 28.47°N, 77.00°E. The crustal model consisted of three layers, appropriate for Peninsular India<sup>23</sup>: layer 1,  $V_P = 5.68$  km,  $V_S = 3.55$  km/s, thickness = 13.8 km; layer 2,  $V_P = 6.16$  km,  $V_S = 3.85$  km/s, thickness = 24.9 km; layer 3,  $V_P = 7.91$  km,  $V_S = 4.65$  km/s, thickness = infinite). A triangular source-time function of 0.5 s duration was taken in the computation. The focal mechanism of the 1960 earthquake was taken to be the

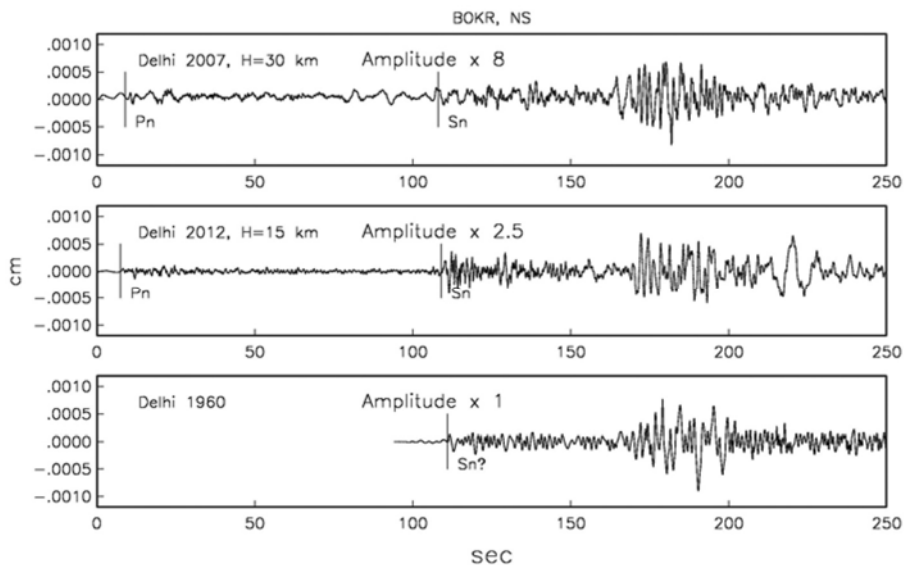


**Figure 2.** Digitized Milne–Shaw displacement seismograms (NS component, bottom trace) of Delhi 1960 earthquake recorded at Bokaro Thermal (BOKR). The high-pass (at 0.1 Hz) NS displacement seismograms of Delhi earthquakes of 2007 and 2012 at BOKR are also shown. *Pn* and *Sn* phases of the 2007 and 2012 are marked. The digitization of 1960 earthquakes begins near the *Sn* arrival. Note that the amplitudes of 2012 and 2007 earthquakes have been multiplied by 2.5 and 8 respectively.

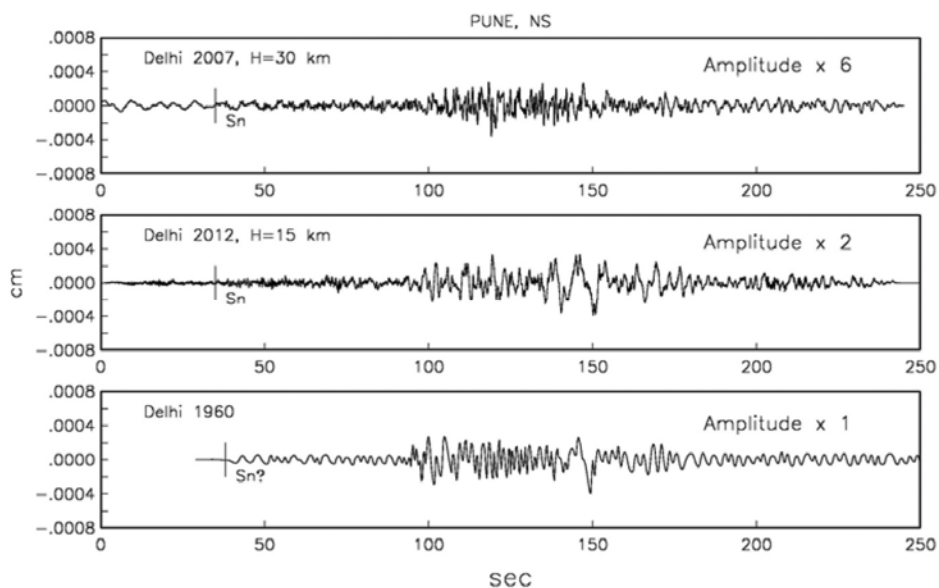


**Figure 3.** Same as Figure 2, but at Poona (PUNE). Note that the amplitudes of 2012 and 2007 earthquakes have been multiplied by 2 and 6 respectively.

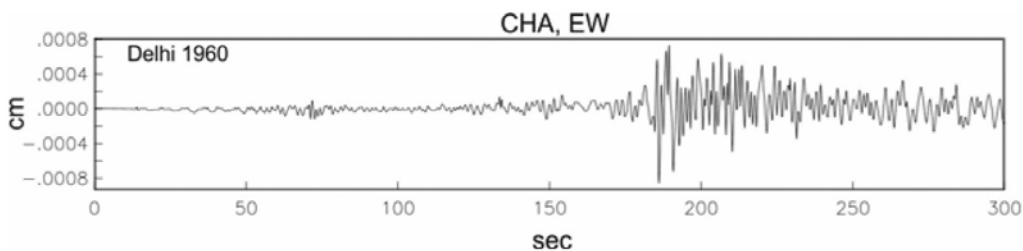


**Figure 4.** Digitized Milne–Shaw EW displacement seismograms of Delhi 1960 earthquake recorded at CHA.

**Table 1.** Calibration earthquakes and  $M_w$  of the 1960 Delhi event estimated from the comparison of long-period levels of displacement spectra at  $R = 1000$  km

Region	Date	Latitude (°N)	Longitude (°E)	Depth (km)	$M_0$ (Nm)	$M_w$	Station used in the analysis/epicentral distance (km)	Delhi 1960 earthquake	
								$M_0$ (Nm)	$M_w$
Bhuj, aftershock	28 January 2001 <sup>a</sup>	23.61	70.46	15	$5.2 \times 10^{17}$	5.74	JBP/970; NDI/907	$1.15 \times 10^{16}$	4.64
Jabalpur	21 May 1997 <sup>b</sup>	23.08	80.06	36	$5.4 \times 10^{17}$	5.75	BHUI/1066; KARD/886	$3.03 \times 10^{16}$	4.92
Bhuj, aftershock	8 February 2001 <sup>c</sup>	23.63	70.45	25	$8.0 \times 10^{16}$	5.20	JBP/972	$1.70 \times 10^{16}$	4.75
Delhi	25 November 2007 <sup>d</sup>	28.57	77.10	30	$1.9 \times 10^{15}$	4.12	BOKR/1012	$1.27 \times 10^{16}$	4.67
Uttarkashi	9 February 2012 <sup>e</sup>	30.99	78.28	6	$1.8 \times 10^{16}$	4.85	BHPL/860; BOKR/1090 BHUI/1212	$1.80 \times 10^{16}$	4.85
Delhi	5 March 2012 <sup>f</sup>	28.73	76.60	15	$9.7 \times 10^{15}$	4.59	BOKR/1012	$1.36 \times 10^{16}$	4.69

<sup>a</sup>Location from IMD; depth and  $M_0$  from Global Centroid Moment Tensor (GCMT) catalogue. <sup>b</sup>Location and depth from Bhattacharya *et al.*<sup>28</sup> and Singh *et al.*<sup>23</sup>;  $M_0$  from GCMT. <sup>c</sup>Singh *et al.*<sup>29</sup>. <sup>d</sup>Singh *et al.*<sup>18</sup>. <sup>e</sup>Location and depth from IMD;  $M_0$  from the present study. <sup>f</sup>Location and depth from IMD;  $M_0$  from the present study.

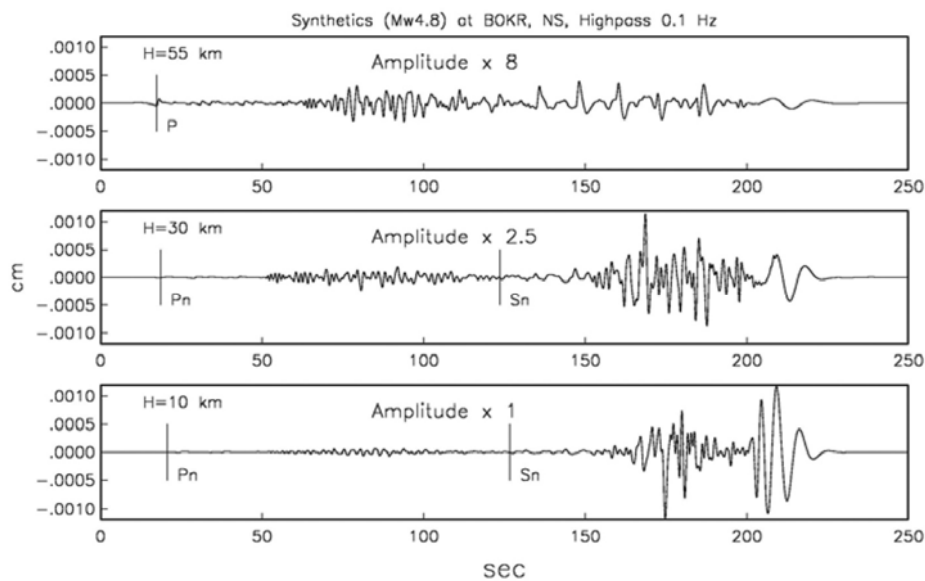


**Figure 5.** Synthetic high-pass (at 0.1 Hz) NS displacement seismograms at BOKR for sources ( $M_w$  4.8) located at depths of 10, 30 and 55 km. See text for other source parameters.  $P_n$  and  $S_n$  phases for source depths of 10 and 30 km, and  $P$  and  $S$  phases for source depth of 55 km are marked. Amplitudes of synthetics corresponding to  $H = 30$  and 55 km have been multiplied by 2.5 and 8 respectively. Note that the origin of the x-axis does not correspond to the origin time of the earthquake.

same as that of the 2012 event, which we determined from first-motion data and regional moment tensor inversion: strike  $36^\circ$ , dip  $54^\circ$  and rake  $-52^\circ$ . High-pass (at 0.1 Hz) NS displacement seismograms at BOKR and PUNE, corresponding to depths of 10, 30, and 55 km are illustrated in Figures 5 and 6. As expected, due to simple crustal structure the synthetic seismograms poorly mimic the observed ones (compare Figure 2 with 5, and Figure 3 with 6). However, the synthetic seismograms rule out a mantle source for the 1960 earthquake.

An approximate estimate of magnitude of the 1960 earthquake can be obtained from comparison of zero to peak amplitudes of the seismograms of the 2007, 2012 and 1960 earthquakes illustrated in Figures 1 and 2. The amplitude of the 1960 earthquake at BOKR is  $\sim 9$  and

three times that of 2007 and 2012 earthquakes respectively. The corresponding value at PUNE is  $\sim 6.7$  and 2 respectively. Since  $M_w$  of the 2007 and 2012 earthquakes is 4.1 and 4.6 (Table 1), the estimated magnitudes of the 1960 earthquake at BOKR and PUNE are 5.1 and 4.9 respectively.

A more reliable estimation of  $M_w$  of the 1960 earthquake consisted of two steps. In the first step we searched for recent, moderate Indian earthquakes (magnitude between 4 and 6) which were recorded at  $R \sim 1000$  km (roughly the hypocentral distance of the stations which produced Milne–Shaw seismograms of the 1960 earthquake) and whose seismic moments  $M_0$  (hence  $M_w$ ) are either known or could be determined. Let us call the selected earthquakes the calibration events. These are listed

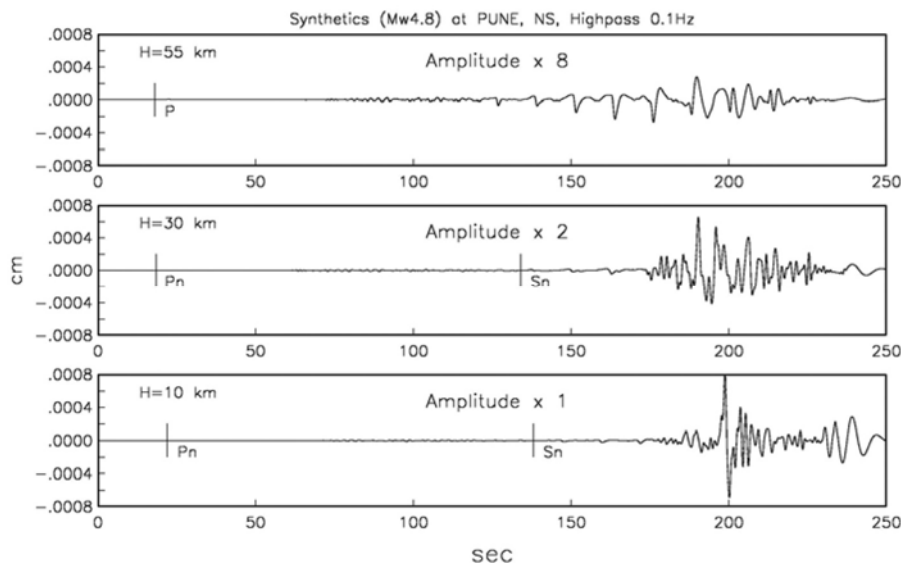


**Figure 6.** Same as Figure 5, but at PUNE. Amplitudes of synthetics corresponding to  $H = 30$  and  $55$  km have been multiplied by 2 and 8 respectively.

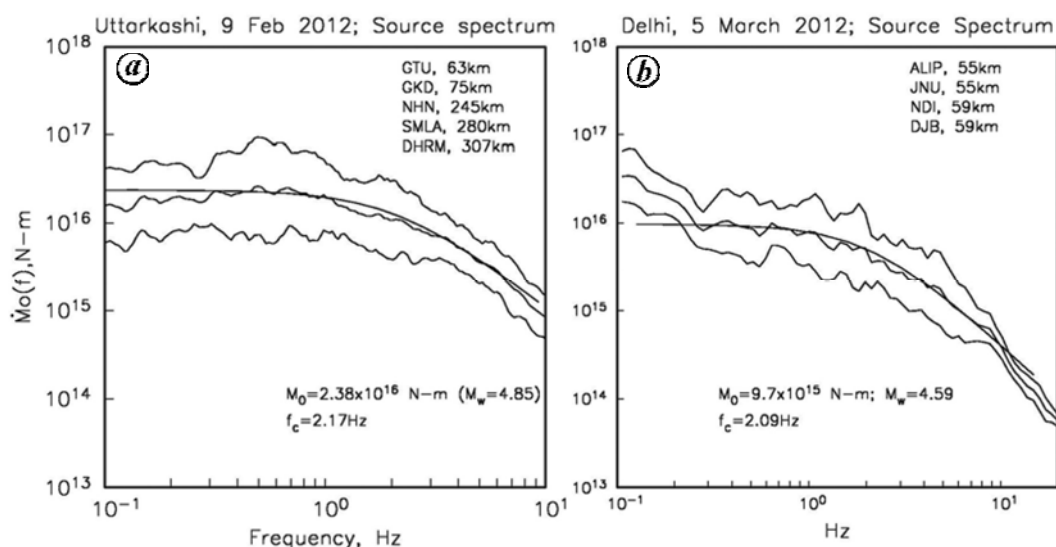


**Figure 7.** Source displacement spectra (median and  $\pm$  one standard deviation curves) of (a) Uttarkashi earthquake of 9 February 2012 and (b) Delhi earthquake of 5 March 2012. The stations (hard sites) used in the analysis and their hypocentral distances are listed. The median spectra are reasonably well fit by Brune’s  $\omega^2$ -source model.  $M_0 = 2.38 \times 10^{16}$  and  $9.70 \times 10^{15}$  N-m for Uttarkashi and Delhi earthquakes respectively.

in Table 1.  $M_0$  of the first four earthquakes is known. We estimated  $M_0$  of the last two earthquakes, which occurred in 2012, from spectral analysis of the  $S$ -wave group. We only used recordings at hard sites. Shear-wave velocity and density at the source were taken as 3.75 km/s and 2.90 g/cm<sup>3</sup> respectively. Singh *et al.*<sup>24</sup> report  $Q(f) = 258f^{0.80}$  for paths along the Himalayan arc and between the arc and Delhi. We used this  $Q$  in the attenuation correction of both the 2012 Uttarkashi and Delhi earthquakes. Geometrical spreading was assumed to be  $1/R$  for  $R < 100$  km and  $1/R^{1/2}$  for  $R \geq 100$  km. Details of the

analysis are given elsewhere<sup>18</sup>. Source displacement spectra of the two earthquakes and  $\omega^{-2}$  source model fitted to the observed median spectra are shown in Figure 7. The low-frequency levels of the spectra directly yield  $M_0$ :  $1.6 \times 10^{16}$  Nm ( $M_w$  4.85) and  $9.7 \times 10^{15}$  Nm ( $M_w$  4.59) for the 2012 Uttarkashi and Delhi earthquakes respectively (Table 1).

In the next step, we selected time windows in the recordings at  $R \sim 1000$  km of each calibration event which included  $Lg$  wave and 80% of the total energy ( $\sim 100$  s). The signals were 5% tapered, fast-Fourier

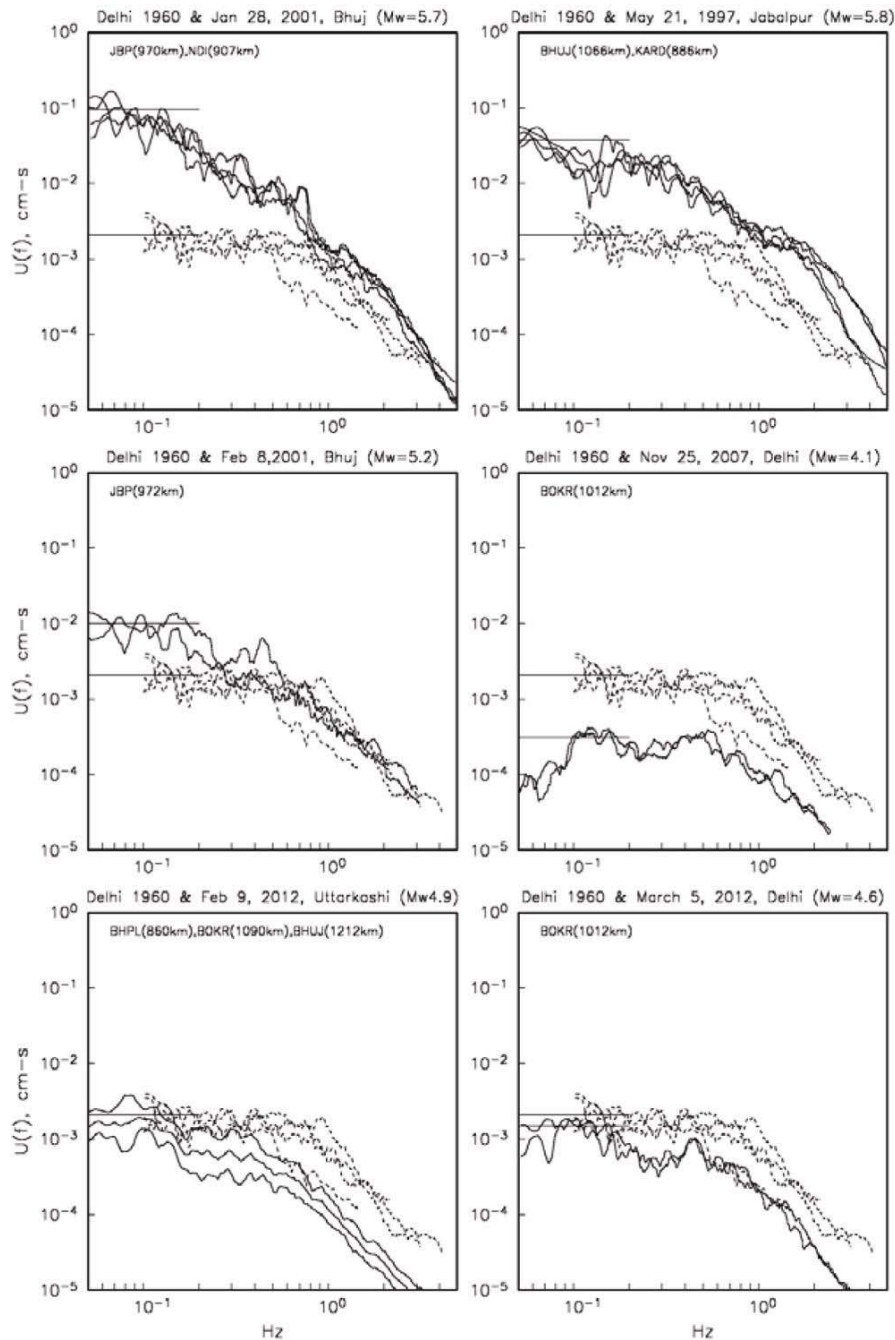


**Figure 8.** Comparison of  $Lg$ -wave spectra of the Delhi 1960 earthquake (dashed curves) with six calibration earthquakes (continuous curves). The recordings used in the analysis are from a distance range 850 to 1250 km (stations and their distances are indicated). The spectra have been reduced to a common distance of 1000 km. For calibration events, the median spectrum and  $\pm$  one standard deviation curves are shown if the number of stations used is  $\geq 3$ ; otherwise the two horizontal-component spectra at each station is shown separately. For the Delhi 1960 event, the spectrum at each station is shown. The spectral level at low frequencies (marked by horizontal line) is proportional to  $M_0$ . Thus,  $M_0$  of the Delhi 1960 earthquake is obtained since its value for the calibration events is known.

transformed, and smoothed by a 1/6 octave-band filter. The spectra were corrected for instrumental response to produce displacement spectra which were then reduced to a common distance  $R$  of 1000 km by assuming that geometrical spreading and anelastic attenuation are given by  $R^{-1/2}$  (surface waves) and  $\exp[-\pi f R/UQ(f)]$  respectively, where  $R$  is the hypocentral distance,  $U$  the group velocity

(taken here as 3.5 km/s),  $f$  the frequency and  $Q(f)$  the quality factor.  $Q(f)$  was taken as  $800f^{0.42}$ , appropriate for paths in the Indian shield<sup>24</sup>. The spectra of the 1960 earthquake were also reduced to  $R = 1000$  km in a similar manner. We note that the corrections were minor since the recordings were in the distance range of 850–1250 km. Figure 8 illustrates the spectra of the Delhi

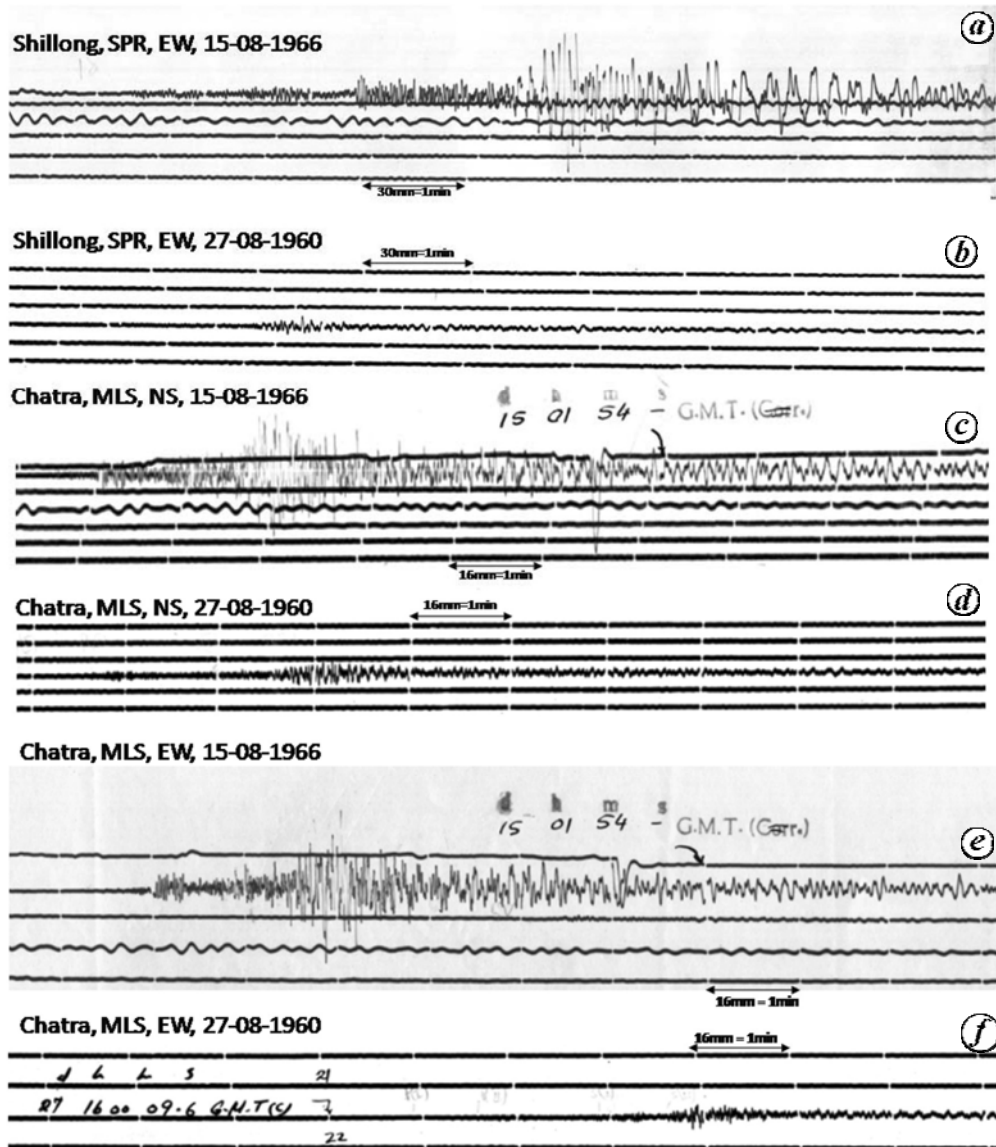


**Figure 9.** Seismograms of 1966 Moradabad and 1960 Delhi earthquakes. *a, b*, Sprengnether EW component at Shillong. *c, d*, Milne–Shaw NS component at Chatra. *e, f*, Milne–Shaw EW component at Chatra.

1960 and the calibration earthquakes. The spectral levels of the 1960 event at low frequencies ( $f < 0.4$  Hz) computed from recordings at different stations are similar ( $\sim 1.27 \times 10^{-3}$  cm-s). However, the spectral fall-off at higher frequencies ( $f > 0.5$  Hz) at PUNE is faster than that at BOKR and CHA. On the other hand, the spectral fall-off in the latter two stations is somewhat unusual compared to those of the calibration events with similar low-frequency spectral level (bottom two frames in Figure 8). This may be due to poor signal-to-noise ratio and errors introduced in the process of digitization of relatively poor quality of the seismograms. Since we are interested in the estimation of  $M_0$ , which is proportional to the low-frequency spectral level, we ignored the inconsistencies at higher frequencies. From Figure 8, we esti-

mated the seismic moment of the 1960 earthquake by comparing the median low-frequency spectral level (0.1–0.2 Hz) of the 1960 event with those of the calibration events (whose  $M_0$  are known). The estimated  $M_0$  ranges between  $1.2$  and  $3.0 \times 10^{16}$  Nm ( $M_w$  4.6–4.9; Table 1). The average  $M_w$  is 4.8.

The Moradabad earthquake of 15 August 1966 occurred when the World-Wide Standard Seismic Network (WWSSN) was fully operational. The ISS bulletin lists its location as  $28.67^\circ\text{N}$ ,  $78.93^\circ\text{E}$ , depth 5 km and magnitude as  $m_b$  5.6. The earthquake occurred about 170 km east of Delhi. Seismographs whose recordings of both the 1966 and 1960 earthquakes are available in the IMD archives are Sprengnether at SHL (EW component) and Milne–Shaw at CHA (both horizontal components). The

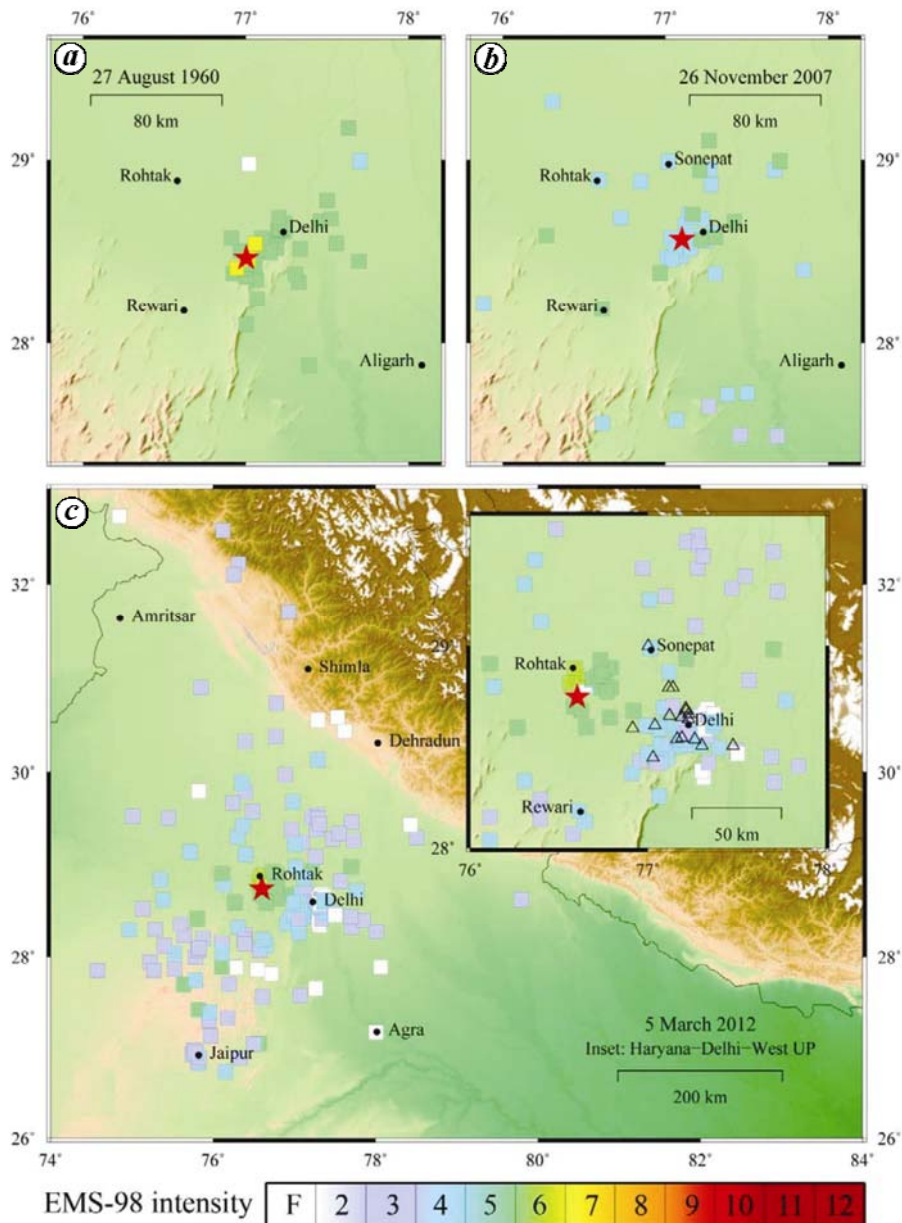


**Figure 10.** EMS-98 intensity distribution of Delhi earthquakes of (a) 1960, (b) 2007 and (c) 2012. Red star indicates instrumental epicentre for the 2007 and 2012 earthquakes; for the 1960 earthquake it indicates centre of maximum intensity contour.

epicentral distances of CHA and SHL are 869 and 1338 km respectively; the corresponding distances from the 1960 epicentre are 1051 and 1510 km. Since the distances differ by a small percentage, the seismograms can be directly compared. Figure 9 shows the EW component of 1966 and 1960 seismograms at SHL and CHA. It is at once clear that the amplitude of the 1960 earthquake is about an order of magnitude smaller than the 1966 earthquake. More precisely, peak-to-peak EW amplitudes at SHL during the 1960 and 1966 earthquakes are 4.2 and 38.0 mm respectively. Assuming that  $m_b$  scales with peak-to-peak amplitude, this yields  $m_b$  4.64 for the 1960

earthquake corresponding to  $m_b$  5.6 for the 1966 earthquake. At CHA, the peak-to-peak amplitudes during the 1960 and 1966 earthquakes are 3.5 and 14.3 mm on the EW component and 3.9 and 18.0 mm on the NW component respectively. This yields  $m_b$  of 4.99 and 4.94. The average  $m_b$  of the three estimations is 4.9, compared to  $M_w$  4.8 estimated above.

The seismic intensity distribution of the 1960 earthquake can also be used to estimate a bound on its magnitude. For this, we used an intensity attenuation relation for the Indian subcontinent developed by Szeliga *et al.*<sup>25</sup> The relation is based on intensities on the European Mac-

roseismic Scale 1998 (EMS-98)<sup>26</sup> reported for Indian earthquakes by Martin and Szeliga<sup>17</sup>. The EMS-98 intensity scale was chosen since it is more adaptable to indigenous construction practices in India. Using the intensity attenuation relation, along with the method of Bakun and Wentworth<sup>27</sup>, Szeliga *et al.*<sup>25</sup> estimated the location and magnitude of historical events of India for which only intensity data were available. For the 1960 earthquake, the intensity magnitude  $M_I$  was 5.7, a value that is rendered incorrect by a cataloguing error in the intensities used in the computation.

To estimate the upper bound of magnitude, we compiled the EMS-98 intensities of the 2007, 2012 and 1960

earthquakes (Figure 10). The earthquakes of 2007 and 2012, whose  $M_w$  are given (Table 1), provide validation for the bounds on  $M_w$  of the 1960 earthquake. The intensity decay plots of these earthquakes are given in Figure 11 (including the median and mean values at each intensity interval). Superimposed on the plots are predicted intensities corresponding to  $M_w$  4, 5 and 6 (eq. (1) and coefficients for cratonic model given in table 1 of Szeliga *et al.*<sup>25</sup>). Note that nearly all median intensities (used in the derivation of intensity prediction equation) for the three earthquakes fall between  $M_w$  4 and 5 curves. Since the instrumentally determined  $M_w$  of 2007 and 2012 events also falls in the 4–5 range, this provides validation of the method, and suggests that  $M_w$  of the 1960 earthquake was also in the range 4–5.

We have shown that the previously reported location, depth and magnitude of the Delhi 1960 earthquake based on instrumental data, field reports and other sources of information are highly inconsistent. A re-examination of the earthquake strongly suggests that it occurred between Delhi Cantonment and Gurgaon (epicentre within ~5 km of 28.47°N, 77.00°E) at a shallow depth ( $\leq 30$  km, but most probably  $\leq 15$  km). The moment magnitude was ~4.8, much less than the magnitude of 6.0 originally reported and often used in seismic hazard estimation.

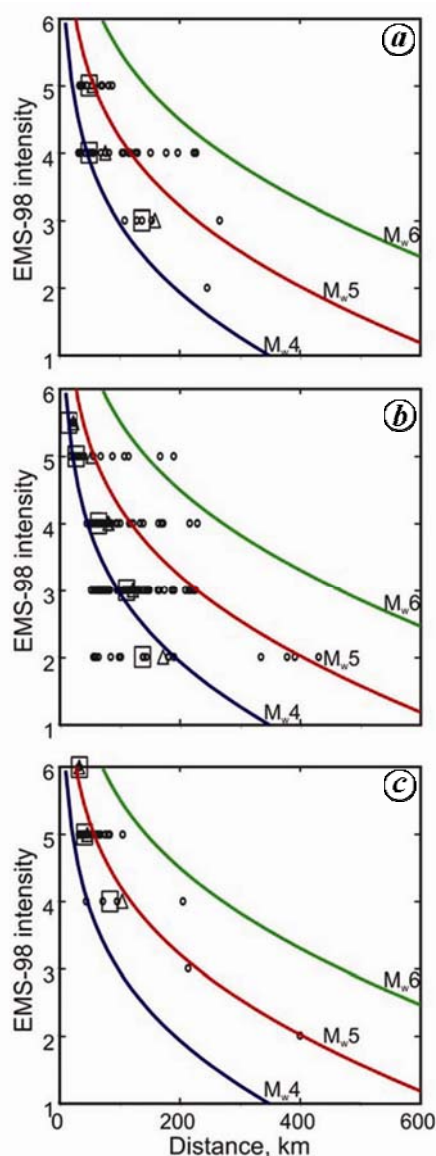


**Figure 11.** EMS-98 intensity as a function of distance for (a) 2007, (b) 2012 and (c) 1960 Delhi earthquakes. Triangles and squares show mean and median intensities respectively, per intensity level. Smooth curves depict predicted intensities for  $M_w$  4, 5 and 6 for cratonic attenuation model<sup>25</sup>. Note that median intensities in almost all cases fall between  $M_w$  4 and 5 curves.

1. Ahmed, K. A., *The Muntakhab al-Lubab of Khafi Khan*, Bibliotheca Indica, Asiatic Society of Bengal, Calcutta, Part II, 1874, pp. 883–885.
2. Oldham, T., A catalogue of Indian earthquakes from the earliest time to the end of AD 1869. *Mem. Geol. Surv. India*, 1883, **29**, 163–215.
3. Bacon, T., *First Impressions and Studies from Nature in Hindostan Embracing an Outline of the Voyage to Calcutta and Five Years' Residence in Bengal and the Doab from 1831 to 1836*, W.H. Allen & Co, London, 1837, vol. 2, pp. 332–333.
4. Bapat, A., Kulkarni, R. S. and Guha, S. K., *Catalogue of Earthquakes in India and Neighbourhood – From Historical Period up to 1979*. Indian Society of Earthquake Technology, Roorkee, 1983.
5. Rao, B. R. and Rao, P. S., Historical seismicity of Peninsular India. *Bull. Seismol. Soc. Am.*, 1984, **74**, 2519–2533.
6. Ambraseys, N. and Jackson, D., A note on early earthquakes in northern India and southern Tibet. *Curr. Sci.*, 2003, **84**, 570–582.
7. Ambraseys, N. and Douglas, J. J., Magnitude calibration of north Indian earthquakes. *Geophys. J. Int.*, 2004, **159**, 165–206.
8. Saha, B. P., On the depth of focus of the Delhi earthquake of 27 August 1960, *Indian J. Meteorol. Geophys.*, 1962, **13**, 137–140.
9. Rothé, J. P., *The Seismicity of the Earth 1953–1965*, UNESCO, Paris, 1969, p. 335.
10. Tandon, A. N. and Srivastava, H. N., Earthquake occurrence in India. In *Earthquake Engineering, Jai Krishna 60th Birth Anniversary Commemoration Volume*, ISET, 1974, pp. 1–47.
11. Iyengar, R. N., Seismic status of Delhi megacity. *Curr. Sci.*, 2000, **78**, 568–574.
12. Iyengar, R. N. and Ghosh, S., Microzonation of earthquake hazard in greater Delhi area. *Curr. Sci.*, 2004, **87**, 1193–1202.
13. Sharma, M. L., Wason, H. R. and Dimri, R., Seismic zonation of the Delhi region for bedrock ground motion. *Pure Appl. Geophys.*, 2003, **160**, 2381–2398.

14. Parvez, I., Vaccari, F. and Panza, G. F., Site-specific microzonation study in Delhi metropolitan city by 2-D modeling of SH and P-SV waves. *Pure Appl. Geophys.*, 2004, **161**, 1165–1185.
15. Parvez, I. A., Vaccari, F. and Panza, G. F., Influence of source distance on site-effect in Delhi city. *Curr. Sci.*, 2006, **91**, 827–835.
16. Nath, M., Narain, K. and Srivastava, J. P., A report on the Delhi earthquake of 27 August 1960, Geological Survey of India, Northern Region, Lucknow, 1960.
17. Martin, S. and Szeliga, W., A catalog of felt intensity data for 570 earthquakes in India from 1636 to 2009. *Bull. Seismol. Soc. Am.*, 2010, **100**, 562–569.
18. Singh, S. K. *et al.*, Delhi earthquake of 25 November 2007 ( $M_w$  4.1): implications for seismic hazard. *Curr. Sci.*, 2010, **99**, 939–947.
19. Michael, A. J., Earthquake sounds. In *Encyclopedia of Solid Earth Geophysics, Seismology* (ed. Gupta, H.), Springer, 2011, pp. 188–191.
20. Hill, D. P., Fischer, F. G., Lahr, K. M. and Coakley, J. M., Earthquake sounds generated by body-wave ground motion. *Bull. Seismol. Soc. Am.*, 1976, **66**, 1159–1172.
21. Pintore, S., Quintiliani, M. and Franceschi, D., Teseo: a vectoriser of historical seismograms. *Comput. Geosci.*, 2005, **31**, 1277–1285.
22. Bouchon, M., The complete synthetics of crustal seismic phases at regional distances, *J. Geophys. Res.*, 1982, **87**, 1735–1741.
23. Singh, S. K., Dattatrayam, R. S., Shapiro, N., Mandal, P., Pacheco, J. F. and Midha, R. K., Crustal and upper mantle structure of the Peninsular India and source parameters of the 21 May 1997, Jabalpur earthquake ( $M_w$  5.8): results from a new regional broadband network. *Bull. Seismol. Soc. Am.*, 1999, **89**, 1631–1641.
24. Singh, S. K., Garcia, D., Pacheco, J. F., Valenzuela, R., Bansal, B. K. and Dattatrayam, R. S.,  $Q$  of the Indian shield. *Bull. Seismol. Soc. Am.*, 2004, **94**, 1564–1570.
25. Szeliga, W., Hough, S. E., Martin, S. and Bilham, R., Intensity, magnitude, location and attenuation in India for felt earthquakes since 1762. *Bull. Seismol. Soc. Am.*, 2010, **100**, 570–584.
26. Gruenthal, G. (ed.), European Macroseismic Scale 1998 (EMS-98), Conseil de l'Europe. *Cahiers Centre Eur. Geodyn. Seismol.*, 1998, **15**.
27. Bakun, W. H. and Wentworth, C. M., Estimating earthquake location and magnitude from seismic intensity data. *Bull. Seismol. Soc. Am.*, 1997, **87**, 1502–1521.
28. Bhattacharya, S. N., Ghose, A. K., Suresh, G., Baidya, P. R. and Saxena, R. C., Source parameters of Jabalpur earthquake of 22 May 1997. *Curr. Sci.*, 1997, **73**, 855–863.
29. Singh, S. K., Pacheco, J. F., Bansal, B. K., Pérez-Campos, X., Dattatrayam, R. S. and Suresh, G., A source study of the Bhuj, India, earthquake of 26 January 2001 ( $M_w$  7.6). *Bull. Seismol. Soc. Am.*, 2004, **94**, 1195–1206.

**ACKNOWLEDGEMENTS.** We thank Andrew Michael for comments on earthquake sounds. Data used in this study were obtained by IMD, IIT-R and WIHG under projects funded by the Ministry of Earth Sciences, Government of India. We acknowledge efforts made by IMD officers in getting the old seismic analogue charts, particularly those of the subject earthquake, scanned and vector digitized through a project implemented by an agency, viz. M/s Society for Automation and Technology Advancement. The research was partly funded by Consejo Nacional de Ciencia y Tecnología (CONACYT), Mexico and Department of Science and Technology (DST), India, under the Indo-Mexican Cooperation Programme in Science and Technology.

Received 9 January 2013; revised accepted 24 May 2013

## Temporal variability in residence time of ambient aerosols using environmental $^{210}\text{Pb}$

Neeraj Rastogi\* and M. M. Sarin

Geosciences Division, Physical Research Laboratory, Ahmedabad 380 009, India

**The regional air quality, atmospheric chemistry and climate change are largely influenced by the chemical composition of ambient aerosols and more importantly, by their residence time on a spatial and temporal scale. The environmental radionuclide  $^{210}\text{Pb}$  ( $t_{1/2} = 22.3$  years), injected into the atmosphere by *in situ* decay of its parent nuclide  $^{222}\text{Rn}$  ( $t_{1/2} = 3.8$  days) from ground sources, is highly particle reactive and thus serves as an ideal tracer to assess the residence time of anthropogenic and natural aerosols from ground-based sources. We report on the temporal variability in residence time of ambient aerosols studied from an urban site (Ahmedabad) and a high altitude site (Mt Abu) in western India. The residence time of aerosols, ranging from ~2 to 8 days, is predominantly controlled by regional meteorology and high dust abundance (shorter removal time) in semi-arid regions. These observations raise the issue of uncertainty in tracing the source region of atmospheric pollutants based on air-mass back trajectory analyses without knowing their actual residence time for a given time-period over a study region.**

**Keywords:** Ambient aerosols, radionuclides, residence time, temporal variability.

AMBIENT aerosols, either emitted directly in particle form (primary particles), or formed in the atmosphere by physico-chemical processes (secondary particles), originate from a variety of natural (sea salt, dust, volcano, etc.) and anthropogenic (fossil fuel and biomass burning) sources. Although the residence time of ambient aerosols in the lower troposphere is reported to be only about a week, their effects from growing anthropogenic sources are increasingly recognized in the deterioration of air quality, atmospheric chemistry and Earth's radiation budget. The residence time of atmospheric aerosols depends upon various removal processes, e.g. dry deposition (by impaction and sedimentation) and wet deposition (by rain, snow). Detailed information of both spatial and temporal variability in the residence time of ambient aerosols is thus essential to understand their atmospheric transport and removal processes.

Atmospheric  $^{210}\text{Pb}$  ( $t_{1/2} = 22.3$  years) together with  $^{222}\text{Rn}$  ( $t_{1/2} = 3.8$  days),  $^{210}\text{Po}$  ( $t_{1/2} = 138$  days) or  $^{210}\text{Bi}$  ( $t_{1/2} = 5$  days) have been used to estimate the residence time of atmospheric aerosols<sup>1–5</sup>. Figure 1 depicts a sche-

\*For correspondence. (e-mail: nrastogi@prl.res.in)